

# The $F^- + CH_3I \rightarrow FCH_3 + I^-$ entrance channel potential energy surface Comparison of electronic structure methods



Rui Sun<sup>a</sup>, Jing Xie<sup>a</sup>, Jiaxu Zhang<sup>b</sup>, William L. Hase<sup>a,\*</sup>

<sup>a</sup> Department of Chemistry and Biochemistry, Texas Tech University, Lubbock, TX 79409, United States

<sup>b</sup> Institute of Theoretical and Simulational Chemistry, Academy of Fundamental and Interdisciplinary Sciences, Harbin Institute of Technology, Harbin 150080, PR China

## ARTICLE INFO

### Article history:

Received 27 February 2014

Received in revised form 17 April 2014

Accepted 18 April 2014

Available online 2 May 2014

### Keywords:

Molecular dynamics simulation  
Nucleophilic substitution reaction  
Ion

## ABSTRACT

The potential energy surface (PES) of the  $F^- + CH_3I \rightarrow FCH_3 + I^-$   $S_N2$  nucleophilic substitution reaction has been studied previously using MP2 and DFT levels of theory (*J. Phys. Chem. A* 2010, 114, 9635–9643). This work indicated that DFT gives a better representation of the PES which has only an hydrogen-bonded entrance channel reaction path, with a hydrogen-bonded transition state  $[F \cdots HCH_2 \cdots I]^-$  connecting the hydrogen-bonded pre-reaction complex  $F^- \cdots HCH_2I$  and  $C_{3v}$  post-reaction complex  $FCH_3 \cdots I^-$ . For the work presented here, CCSD(T) with three different basis set and two effective core potentials (i.e. PP/d, PP/t and ECP/d) was employed to investigate stationary point properties for this reaction. Besides the hydrogen-bonded entrance channel stationary points, CCSD(T) also predicts a traditional  $C_{3v}$  transition state  $[F \cdots CH_3 \cdots I]^-$  connecting a  $C_{3v}$  pre-reaction complex  $F^- \cdots CH_3I$  with the  $C_{3v}$  post-reaction complex  $FCH_3 \cdots I^-$ . Though CCSD(T) gives a  $CH_3F \cdots I^-$  binding energy and  $CH_3F$  and  $CH_3I$  geometries in almost exact agreement with experiment, it gives a heat of reaction  $\sim 20$  kJ/mol less exothermic than experiment. The MP2 PES for this reaction, determined in the previous study, is very similar to the CCSD(T), but obtained with a much smaller computational cost. Direct dynamics simulations for the  $F^- + CH_3I \rightarrow FCH_3 + I^-$  reaction are feasible with MP2.

© 2014 Elsevier B.V. All rights reserved.

## Introduction

The traditional potential energy surface (PES) for a  $X^- + CH_3Y \rightarrow XCH_3 + Y^-$   $S_N2$  reaction has an ion-dipole  $X^- \cdots CH_3Y$  pre-reaction complex, a  $[X \cdots CH_3 \cdots Y]^-$  central barrier, and an ion-dipole  $XCH_3 \cdots Y^-$  post-reaction complex [1–9]. If X and Y are halogen-atoms, these structures have  $C_{3v}$  symmetry for the traditional PES. Non-traditional PESs without  $C_{3v}$  symmetry are found if the  $X^-$  and/or  $Y^-$  nucleophiles are not halide ions [9–11]. An example is the  $OH^- + CH_3F$   $S_N2$  reaction which has a traditional  $OH^- \cdots CH_3F$  pre-reaction complex, but for the  $CH_3OH \cdots F^-$  post-reaction complex  $F^-$  is hydrogen-bonded to the  $-OH$  moiety [9].

In recent work [12], different electronic structure theories and basis sets were used to investigate the PES for the  $F^- + CH_3I \rightarrow FCH_3 + I^-$   $S_N2$  reaction. The theoretical methods included second order Møller–Plesset perturbation theory (MP2) [13], DFT [14] with the OPBE [15], OLYP [16], HCTH407 [17], BhandH [18], and B97-1 [19] functionals, and the coupled-cluster method

with single and double excitations and perturbed triple excitations, i.e. CCSD(T), for single point calculations. Both the aug-cc-pVDZ [20,21] and aug-cc-pVTZ [20,21], double- and triple-zeta, basis sets were used, along with pseudo potentials and augmented basis sets for the I-atom [12]. Of particular interest is that MP2 and DFT give different forms of the entrance-channel PES for this reaction, as shown in Fig. 1. For the DFT/B97-1/ECP/d PES there are only a hydrogen-bonded  $F^- \cdots HCH_2I$  pre-reaction complex and a hydrogen-bonded  $[F \cdots HCH_2 \cdots I]^-$  transition state (TS). In contrast, the MP2/ECP/t PES has these stationary point structures as well as the traditional  $F^- \cdots CH_3I$  ion-dipole complex and  $[F \cdots CH_3 \cdots I]^-$  TS, both with  $C_{3v}$  structures. The DFT PES and energetics in Fig. 1 are from the B97-1 functional, but other DFT functionals give similar results. Only the BhandH functional, and only with the double-zeta basis set, did a DFT theory give a PES somewhat akin to that found with MP2.

In this previous study [12], single-point CCSD(T)/complete basis set extrapolation (CBS) calculations were performed [12] to assess the accuracy of the MP2 and DFT calculations of the entrance channel stationary points for the  $F^- + CH_3I \rightarrow FCH_3 + I^-$  PES. The MP2 potential energy curve, connecting the MP2  $C_{3v}$   $F^- \cdots CH_3I$  complex and  $C_{3v}$   $[F \cdots CH_3 \cdots I]^-$  TS, was calculated. The resulting MP2/PP/d

\* Corresponding author.

E-mail address: [bill.hase@ttu.edu](mailto:bill.hase@ttu.edu) (W.L. Hase).

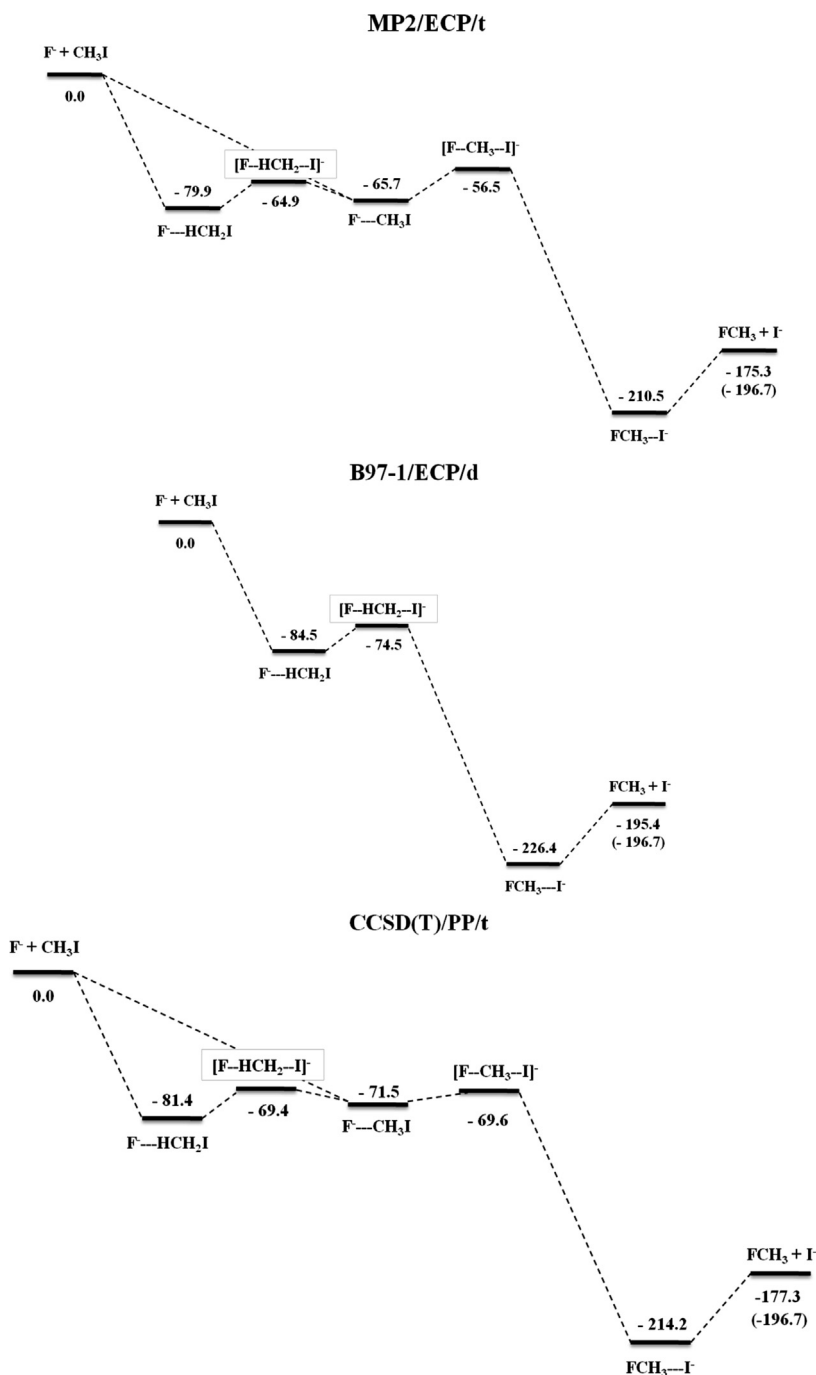


**Fig. 1.** Potential energy curves and stationary points for the MP2/ECP/t, B97-1/ECP/d and CCSD(T)/PP/t PESs for the  $F^- + CH_3I \rightarrow FCH_3 + I^-$   $S_N2$  reaction. The energies in kJ/mol are relative to the reactants, and are at 0 K and do not include ZPEs. The experimental enthalpy of reaction at 0 K corrected to remove zero-point energy is in parentheses.

barrier from the complex to the TS is 2.5 kJ/mol. In contrast to this MP2 barrier, the CCSD(T)/CBS single point calculations give an energy for the MP2 TS which is 0.8 kJ/mol lower in energy than the MP2 complex. Hence, the CCSD(T) single point calculations suggest the  $C_{3v}$   $[F \cdots CH_3 \cdots I]^-$  TS structure is not a stationary point on the actual PES.

In the work presented here the CCSD(T) theory is used to investigate the entrance channel of the  $F^- + CH_3I \rightarrow FCH_3 + I^-$  PES. CCSD(T), with different basis sets, is used to optimize structures for stationary points in the entrance channel, including TSs. Section II describes the computational methodology and the results of the calculations are presented in Section III. The article concludes with a Summary.

### Computational methodology

CCSD(T) theory was employed to determine accurate stationary point properties for the reactants, pre-reaction complexes, transition states, and products on the  $F^- + CH_3I \rightarrow FCH_3 + I^-$  PES. Three basis sets, called ECP/d, PP/d, and PP/t were used in the calculations. Their details were described in previous work [12] and presented here as well. The ECP/d basis set is the combination of Dunning and Woon's aug-cc-pVDZ basis set [20,21] for the C, H, and F atoms and the Wadt and Hay effective core potential [22] (ECP) for the core electrons, and a 3s, 3p basis sets for the valence electrons, which were augmented by a d-polarization function with an 0.262 exponent, and s, p, and d diffuse functions with exponents of 0.034,

0.039, and 0.0873 for I [23]. For the PP/d and PP/t basis sets, the double-(d) and triple-(t)  $\zeta$  basis sets, aug-cc-pVDZ and aug-cc-pVTZ [20,21], were used for the C, H, and F atoms. However, the Peterson aug-cc-pVDZ and aug-cc-pVTZ basis sets, with a pseudopotential (PP) [24], were used for iodine. The only difference between ECP/d and PP/d is the treatment of iodine. The ECP/d basis set is adapted from Wadt and Hay ECP [22], which considers the outmost *s* and *p* orbitals as valence electrons (neglecting 40 core electrons) and derived from an all-electron numerical relativistic Hartree-Fock atomic wavefunction and fit to an analytical representation for use in molecular calculations. This basis set was further modified by Hu and Truhlar for the distortion of CH<sub>3</sub>I and ion-dipole precursor complex [23], with an augmented polarization function added. For the PP/d basis set, the 28 inner-core electrons of iodine (1s–3d) are replaced by an energy-consistent pseudopotential, which is optimized in a multiconfigurational Dirac-Hartree-Fock calculation. Relativistic effects for iodine are considered in both ECP/d and PP/d. The more recent PP/d basis set contains a larger number of basis functions and therefore calculations with it are more computationally expensive.

Quasi-Newton optimization with line searches and an approximate energy Hessian update algorithm were used for the geometry optimizations (energy minimum and transition state search) [25]. As shown in Fig. 1, the MP2/ECP/t entrance channel has a very flat potential energy curve, with 4 stationary point structures (i.e., 2 potential energy minima and 2 transition states) with differences in potential energy of  $\sim 20$  kJ/mol or less. Therefore, initial geometries for the stationary point calculations were crucial for the CCSD(T) optimizations. The MP2/PP/t geometries from reference 12 were used as the initial geometries. Using the line search option guaranteed the geometry optimization calculation ended within a very small region near the PES minimum [26]. Then the optimization was restarted using a very small trust radius and convergence criteria. The CCSD(T) triple  $\zeta$  basis set calculations were very computationally expensive and the average cost for one geometry update, during the optimization, was about 5 h for a 240-core MPI machine (480 cores had to be allocated for more memory demand). The computer program used for the work presented here is NWChem (version 6.1) [27].

## Results and discussion

Fig. 1 shows the F<sup>−</sup> + CH<sub>3</sub>I entrance channel PES obtained from CCSD(T) with the PP/t basis set. CCSD(T) gives a PES similar to that for MP2. In particular, there is a hydrogen-bonded F<sup>−</sup>⋯HCH<sub>2</sub>I pre-reaction complex, a transition state connecting this complex with the traditional C<sub>3v</sub> pre-reaction complex F<sup>−</sup>⋯CH<sub>3</sub>I, and then a TS connecting this complex to the C<sub>3v</sub> post-reaction complex FCH<sub>3</sub>⋯I<sup>−</sup>. Molecular structures of the potential energy minima and transition states for both the C<sub>3v</sub> and hydrogen-bonded entrance channels are depicted in Fig. 2.

In Table 1, CCSD(T) energies for the PP/t, PP/d and ECP/d basis sets are compared. Also included are the MP2 energies with the ECP/d, ECP/t, PP/d, and PP/t basis sets. The CCSD(T)/PP/t energy barrier from the pre-reaction complex to the transition state is 1.9 kJ/mol for the C<sub>3v</sub> channel and 12.0 kJ/mol for the hydrogen-bonded channel. It is of interest to investigate the effect of the basis set size on the PES. Therefore, CCSD(T) calculations were performed using the smaller PP/d basis set with the same pseudopotential. CCSD(T)/PP/d gives a very similar PES to that of CCSD(T)/PP/t. For example, the CCSD(T)/PP/t potential energy release from reactants to pre-reaction complex, for the C<sub>3v</sub> and hydrogen-bonded reaction channel, is 71.5 and 81.4 kJ/mol, respectively. For comparison, the corresponding CCSD(T)/PP/d values are 74.2 and 82.6 kJ/mol. Also, CCSD(T)/PP/d yields a reaction barrier (from pre-reaction complex

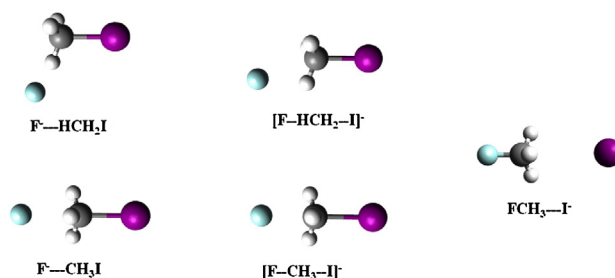


Fig. 2. Molecular structures of potential energy minima and transition states for the C<sub>3v</sub> and hydrogen-bonded entrance channel reaction paths for the F<sup>−</sup> + CH<sub>3</sub>I → FCH<sub>3</sub> + I<sup>−</sup> S<sub>N</sub>2 reaction. For the hydrogen-bonded reaction path H1 is the H atom that's closer to F, and H2 is one of the other 2 atoms.

to the corresponding transition state) only 1.9 and 0.4 kJ/mol lower than the CCSD(T)/PP/t value for C<sub>3v</sub> and hydrogen-bonded pathways, respectively.

The geometries of the CCSD(T) stationary points with the ECP/d, PP/d, and PP/t basis sets are give in Table 2, where they are compared with the MP2 geometries as well as experimental geometries. For the CCSD(T) calculations the ECP/d and PP/d geometries are very similar as found previously [12] for the MP2 calculations. The principal difference between the geometries is that PP/t gives shorter bond lengths than PP/d does. A comparison of MP2/ECP/d and MP2/ECP/t geometries gives the same result [12]. The MP2 and CCSD(T) geometries are in overall good agreement with experiment.

The ECP/d double zeta basis set [28], which is similar to PP/d but with a different number of core electrons, was used to investigate the effect of different core potentials. The CCSD(T)/ECP/d hydrogen-bonded entrance channel is almost the same as that obtained from CCSD(T)/PP/t and CCSD(T)/PP/d. However, only the C<sub>3v</sub> pre-reaction complex was found with CCSD(T)/ECP/d theory, the C<sub>3v</sub> transition state was not found.

As reported previously [12], MP2 predicts both C<sub>3v</sub> and hydrogen-bonded reaction pathways with the ECP/d, ECP/t, PP/d and PP/t basis sets. The MP2 PESs are overall independent of the basis set, with the exception that MP2/ECP/t gives a higher barrier for the C<sub>3v</sub> pathway. The PESs from MP2/ECP/d and MP2/PP/d have the best agreement with CCSD(T)/PP/t. The relative energies for all the critical points (energy minima and transition states) from those two levels of theory are only  $\sim 3$  kJ/mol higher than the values from CCSD(T)/PP/t. Considering the computational expense, MP2/ECP/d, with the smallest number of basis functions, could serve as the electronic structure theory method for future direct dynamic simulations. The B97-1/ECP/d single point energies are  $-76.73$  and  $-82.37$  kJ/mol, respectively, for the C<sub>3v</sub> stationary points F<sup>−</sup>⋯CH<sub>3</sub>I and [F⋯CH<sub>3</sub>⋯I]<sup>−</sup> optimized with CCSD(T)/PP/t.

The F<sup>−</sup> + CH<sub>3</sub>I → FCH<sub>3</sub> + I<sup>−</sup> reaction is highly exothermic due to the strong binding between the fluorine and carbon atoms in the product molecule, CH<sub>3</sub>F. Using the latest thermal chemistry data [29–31], the heat of reaction for F<sup>−</sup> + CH<sub>3</sub>I → FCH<sub>3</sub> + I<sup>−</sup> at 0 K is  $-189.74 \pm 0.31$  kJ/mol. The respective zero point energies for CH<sub>3</sub>I and CH<sub>3</sub>F from CCSD(T)/ECP/d after anharmonic corrections [32] are 95.29 and 102.23 kJ/mol. The corresponding experimental values are 95.72 and 103.96 kJ/mol, from work by Duncan et al. [33] and Law et al. [34]. If the CCSD(T)/ECP/d zero-point energies, with anharmonic corrections, are used to remove zero-point energy from the experimental enthalpy of reaction at 0 K, the resulting enthalpy is  $-196.68$  kJ/mol which may be compared with the theoretical electronic energies. This comparison is made in Table 1, where it is seen that CCSD(T) substantially underestimates the reaction exothermicity by about 20 kJ/mol. The MP2 calculations predict a similar result as CCSD(T). It is possible that the difference

**Table 1**  
CCSD(T) and MP2 stationary point energies for the  $F^- + CH_3I$   $S_N2$  reaction.<sup>a</sup>

Basis set	Stationary point					
	$F^- \cdots HCH_2I$	$F^- \cdots CH_3I$	$[F \cdots HCH_2 \cdots I]^-$	$[F \cdots CH_3 \cdots I]^-$	$FCH_3 \cdots I^-$	$CH_3F + I^-$
	MP2 <sup>b</sup>					
ECP/d	-79.1	-68.2	-66.1	-65.3	-208.8	-172.4
ECP/t	-79.9	-65.7	-64.9	-56.5	-210.5	-175.3
PP/d	-79.5	-69.0	-67.4	-66.5	-211.7	-174.9
PP/t	-82.0	-69.0	-67.4	-63.6	-208.8	-171.1
	CCSD(T)					
ECP/d	-82.2	-72.8	-69.8	- <sup>c</sup>	-214.0	-176.7
PP/d	-82.6	-74.2	-71.0	-74.2	-217.7	-180.5
PP/t	-81.4	-71.5	-69.4	-69.6	-214.2	-177.3
expt. <sup>d</sup>						-196.7

<sup>a</sup> Energies are in kJ/mol with respect to the  $F^- + CH_3I$  reactants, and are at 0 K without zero point energies.

<sup>b</sup> Energies for the MP2 calculations are obtained from Supporting Information in ref. [12]. The energies are electronic energies without ZPE.

<sup>c</sup> A  $C_{3v}$   $[F \cdots CH_3 \cdots I]^-$  TS was not found with the CCSD(T)/ECP/d calculations.

<sup>d</sup> Experimental enthalpy of reaction at 0 K corrected to remove zero-point energy, see text.

between the CCSD(T) and experimental heats of reaction may rise from the incompleteness of the representation of the one particle basis and that of the n-particle correlation treatment in the calculations. As shown in Fig. 1, B97-1/ECP/d gives a heat of formation of 195.4 kJ/mol and in excellent agreement with experiment.

The experimental  $FCH_3$  and  $I^-$  binding energy was used to compare with the electronic structure calculations. It has been previously reported that complexation energies of  $X^- \cdots CH_3Y$  ( $X, Y = F,$

Cl, Br and I) complexes depend primarily on the identity of  $X^-$  and to a much smaller extent on the identity of Y in the  $CH_3Y$  molecule [35]. Therefore the complexation energy of  $FCH_3$  and  $I^-$  should be similar to, but possibly somewhat smaller than, that for  $ICH_3$  and  $I^-$  [36]. The experimental binding energy (at 0 K) for  $ICH_3$  and  $I^-$  was reported to be  $\sim 35$  kJ/mol [12,35,36], which is only 2.3, 2.2 and 1.9 kJ/mol less than the  $FCH_3$  and  $I^-$  binding energy found from the CCSD(T) calculations with ECP/d, PP/d and PP/t, respectively.

**Table 2**  
MP2 and CCSD(T) stationary point geometries for the  $F^- + CH_3I$   $S_N2$  reaction<sup>a</sup>.

Basis set	R(C-F)	R(C-I)	R(C-H)	R(F-H)	A(H-C-H)	A(I-C-H)
	$F^- + CH_3I$					
ECP/d	-	2.143 (2.160) <sup>b</sup>	1.094 (1.098)	-	111.1 (111.2)	108.0 (107.7)
ECP/t	-	2.112	1.079	-	110.9	108.3
PP/d	-	2.149 (2.166)	1.095 (1.099)	-	111.1 (111.3)	107.7 (107.6)
PP/t	-	2.117 (2.134)	1.080 (1.085)	-	111.0 (111.2)	107.9 (107.7)
Exp. <sup>c</sup>	-	2.132	1.084	-		107.7
	$F^- \cdots CH_3I$					
ECP/d	2.433 (2.339)	2.228 (2.296)	1.088 (1.089)	2.377 (2.333)	112.8 (114.5)	105.9 (103.8)
ECP/t	2.489	2.167	1.074	2.394	111.3	107.6
PP/d	2.424 (2.237)	2.234 (2.355)	1.088 (1.088)	2.372 (2.279)	112.9 (116.1)	105.8 (101.5)
PP/t	2.419 (2.383)	2.185 (2.227)	1.074 (1.708)	2.353 (2.339)	112.4 (113.2)	106.4 (105.3)
	$[F \cdots CH_3 \cdots I]^-$					
ECP/d	2.153 (-)	2.375 (-)	1.083 (-)	2.245	117.3	99.5 (-)
ECP/t	2.064	2.381	1.067	2.188	118.2	98
PP/d	2.150 (2.230)	2.377 (2.351)	1.083 (1.088)	2.242 (2.291)	117.3 (116.6)	99.4 (100.8)
PP/t	2.068 (2.143)	2.371 (2.366)	1.068 (1.074)	2.189 (2.232)	118.1 (117.3)	98.1 (99.5)
	$FCH_3 \cdots I^-$					
ECP/d	1.433 (1.435)	3.585 (3.573)	1.094 (1.098)	2.061 (2.066)	110.4 (110.4)	71.5 (70.8)
ECP/t	1.406	3.598	1.08	2.033	109.9	70.9
PP/d	1.433 (1.437)	3.577 (3.571)	1.094 (1.099)	2.061 (2.068)	110.4 (110.4)	71.5 (71.5)
PP/t	1.410 (1.414)	3.522 (3.549)	1.082 (1.087)	2.036 (2.044)	110.0 (110.0)	71.1 (70.8)
	$FCH_3 + I^-$					
ECP/d	1.407 (1.409)	-	1.097 (1.102)	2.039 (2.056)	110.6 (111.4)	-
ECP/t	1.382	-	1.083	2.013	110.1	-
PP/d	1.407 (1.410)	-	1.097 (1.103)	2.039 (2.045)	110.6 (110.6)	-
PP/t	1.385 (1.389)	-	1.085 (1.090)	2.014 (2.022)	110.2 (110.2)	-
Exp. <sup>c</sup>	1.382	-	1.095			-
Basis set	R(C-F)	R(C-I)	R(F-H1)	R(C-H1)	A(F-C-I)	A(H2-C-H1)
	$F^- \cdots HCH_2I$					
ECP/d	2.712 (2.709)	2.169 (2.193)	1.574 (1.571)	1.147 (1.147)	115.4 (115.3)	113.2 (113.6)
ECP/t	2.68	2.13	1.55	1.136	114.8	112.5
PP/d	2.711 (2.708)	2.174 (2.199)	1.574 (1.571)	1.146 (1.148)	115.7 (115.8)	113.3 (113.8)
PP/t	2.691 (2.692)	2.135 (2.159)	1.566 (1.565)	1.133 (1.138)	115.3 (115.9)	112.8 (113.2)
	$[F \cdots HCH_2 \cdots I]^-$					
ECP/d	2.574 (2.551)	2.195 (2.225)	2.094 (2.004)	1.092 (1.095)	160.4 (158.9)	111.0 (111.6)
ECP/t	2.556	2.153	2.09	1.076	163.6	110.2
PP/d	2.568 (2.557)	2.201 (2.228)	2.045 (1.998)	1.092 (1.096)	160.4 (158.4)	111.1 (111.5)
PP/t	2.538 (2.538)	2.161 (2.184)	2.046 (2.015)	1.078 (1.083)	161.7 (160.1)	110.7 (111.1)

## Summary

In the work presented here, properties of stationary points on the entrance channel PES for the  $F^- + CH_3I \rightarrow FCH_3 + I^-$   $S_N2$  reaction were investigated by CCSD(T) theory with different basis sets and effective core potentials. The CCSD(T) PES is found to be in very good agreement with the PES obtained previously from MP2 calculations [12], which contains both the traditional  $C_{3v}$  and hydrogen-bonded reaction paths. The experimental enthalpy of reaction at 0 K corrected to remove zero-point energy is  $-196.68$  kJ/mol and about 20 kJ/mol lower than the result from the CCSD(T)/PP/t calculation. This difference between experiment and calculation is substantial. In contrast, the calculated  $FCH_3$  and  $I^-$  binding energy is in much better agreement with experiment. The  $FCH_3 \cdots I^-$  and  $I CH_3 \cdots I^-$  complexation energies are expected to be quite similar [35]. The CCSD(T)/PP/t value for the former is 36.9 kJ/mol and in good agreement with the experimental value for the latter of  $\sim 35$  kJ/mol [36]. The MP2 binding energy is nearly the same as that for CCSD(T).

It is possible that a more accurate CCSD(T) heat of reaction would be obtained if larger basis sets were used and the enthalpy extrapolated to the complete basis set (CBS) limit [37]. In addition different pseudopotentials for the I-atom could be considered.

An important feature of  $F^- + CH_3I \rightarrow FCH_3 + I^-$  reaction is the relatively flat entrance channel PES. For the highest level of theory reported here, CCSD(T)/PP/t, the energies for the  $F^- \cdots HCH_2I$  and  $F^- \cdots CH_3I$  complexes, relative to the reactants, are  $-81.4$  and  $-71.5$  kJ/mol, respectively. The former connects to a hydrogen-bonded TS via a barrier of 12.0 kJ/mol, while the latter connects to a  $C_{3v}$  TS via a barrier of only 1.9 kJ/mol. Moving from these TSs to the  $C_{3v}$  post-reaction complex  $FCH_3 \cdots I^-$ , the system releases  $\sim 145$  kJ/mol of energy. Hence, reaction entrance channel is much flatter, which may have important implications for the reaction dynamics. MP2 theory with the ECP/d and PP/d basis sets reproduces the CCSD(T) region of PES very well. The MP2 PES is only shifted up from the CCSD(T) PES by  $\sim 3$  kJ/mol, with both hydrogen-bonded and  $C_{3v}$  barriers remaining the same.

In previous work [38], direct dynamics simulations were performed for the  $F^- + CH_3I \rightarrow FCH_3 + I^-$   $S_N2$  reaction at collision energies of 0.32 and 1.53 eV, using DFT/B97-1/ECP/d to represent the PES. At 0.32 eV the scattering angle distribution and the distribution of internal energy in reaction product  $CH_3F$ , determined from the simulations, are in good agreement with the experimental distributions. The only difference is in the scattering angle distribution and, compared to the experiments, there is slightly more forward scattering and less backward scattering in the simulations. At 1.53 eV the difference between experiment and simulation is more substantial. The simulation gives an average product internal energy in agreement with experiment, but the simulation distribution is narrower than that found experimentally. The simulation gives substantially more forward scattering and less backward scattering compared to the experimental results. Overall, better agreement is found between experiment and simulation at the lower collision energy.

The result of the current work is that the stationary points on the MP2 PES agree with those for the high-level CCSD(T) PES, while the B97-1/ECP/d PES disagrees with the CCSD(T) PES. It might be expected that this difference would manifest itself at low collision energies. However, at a 0.32 eV collision energy the dynamics given by the B97-1/ECP/d PES are in overall good agreement with experiment. It is at the higher collision energy of 1.53 eV where the difference in the B97-1/ECP/d and experimental dynamics become more significant. Apparently there are high energy regions of the B97-1/ECP/d PES which are inaccurate, giving rise to inaccurate reaction dynamics at high collision energies. The previous study [12] indicated that the OPBE, OLYP, HCTH407, and BhandH functionals give a  $F^- + CH_3I \rightarrow FCH_3 + I^-$  PES similar to that obtained

with B97-1. In future work it will be important to determine if there are DFT functionals which give a PES for this reaction in agreement with that found with CCSD(T). Functionals which could be considered include B3LYP [39], BPW91 [40,41], and M06-2x [42].

It is of interest to study the  $F^- + CH_3I \rightarrow FCH_3 + I^-$   $S_N2$  reaction dynamics with a MP2 PES and such direct dynamics are in progress. Finally in assessing differences between the B97-1/ECP/d and experimental reaction, classical trajectory direct dynamics are expected to be accurate at the high collision energy of 1.53 eV [10].

## Acknowledgements

This material is based upon work supported by the Robert A. Welch Foundation under grant D-0005. The authors acknowledge the Texas Advanced Computing Center (TACC) at The University of Texas at Austin for providing HPC resources that have contributed to the research results reported within this paper (URL: <http://www.tacc.utexas.edu>). Jiayu Zhang acknowledges financial support from the Institute of Chemistry, Chinese Academy of Sciences (No. CMS-PY-201316). Support was also provided by the High-Performance Computing Center (HPCC) at Texas Tech University (TTU), under the direction of Philip W. Smith, and the TTU Department of Chemistry & Biochemistry cluster Robinson, whose purchase was funded by the National Science Foundation under the CRIF-MU Grant No. CHE-0840493. The authors also wish to thank Branko Ruscic for helpful comments.

## References

- [1] C.A. Lieder, J.I. Brauman, Detection of neutral products in gas-phase, ion-molecule reactions, *J. Am. Chem. Soc.* 96 (1974) 4028–4030.
- [2] W.N. Olmstead, J.I. Brauman, Gas-phase nucleophilic displacement reactions, *J. Am. Chem. Soc.* 99 (1977) 4219–4228.
- [3] W.L. Hase, Simulations of gas-phase chemical reactions: applications to  $S_N2$  nucleophilic substitution, *Science* 266 (1994) 998–1002.
- [4] G.H. Peslherbe, H.B. Wang, W.L. Hase, Trajectory studies of  $S_N2$  nucleophilic substitution 5. semiempirical direct dynamics of  $Cl^- \cdots CH_3Br$  unimolecular decomposition, *J. Am. Chem. Soc.* 118 (1996) 2257–2266.
- [5] H.B. Wang, W.L. Hase, Kinetics of  $F^- + CH_3Cl$   $S_N2$  nucleophilic substitution, *J. Am. Chem. Soc.* 119 (1997) 3093–3102.
- [6] M.L. Chabiny, S.L. Craig, C.K. Regan, J.I. Brauman, Gas-phase ionic reactions: dynamics and mechanism of nucleophilic displacements, *Science* 279 (1998) 1882–1886.
- [7] J.M. Gonzales, R.S. Cox III, S.T. Brown, W.D. Allen, H.F. Schaefer III, Assessment of density functional theory for model  $S_N2$  reactions:  $CH_3X + F^-$  ( $X = F, Cl, CN, OH, SH, NH_2, PH_2$ ), *J. Phys. Chem. A* 105 (2001) 11327–11346.
- [8] J.K. Laerdahl, E. Uggerud, Gas phase nucleophilic substitution, *Int. J. Mass Spectrom.* 214 (2002) 277–314.
- [9] L. Sun, K. Song, W.L. Hase, A  $S_N2$  reaction that avoids its deep potential energy minimum, *Science* 296 (2002) 875–878.
- [10] P. Manikandan, J. Zhang, W.L. Hase, Chemical dynamics simulations of  $X^- + CH_3Y \rightarrow XCH_3 + Y^-$  gas-phase  $S_N2$  nucleophilic substitution reactions. Nonstatistical dynamics and nontraditional reaction mechanisms, *J. Phys. Chem. A* 116 (2012) 3061–3080.
- [11] R. Otto, J. Xie, J. Brox, S. Trippel, M. Stei, T. Best, M.R. Siebert, W.L. Hase, R. Westen, Reaction dynamics of temperature-variable anion water clusters studied with crossed beams and by direct dynamics, *Faraday Discuss. Chem. Soc.* 157 (2012) 41–57.
- [12] J. Zhang, W.L. Hase, Electronic structure theory study of the  $F^- + CH_3I \rightarrow FCH_3 + I^-$  potential energy surface, *J. Phys. Chem. A* 114 (2010) 9635–9643.
- [13] C.M. Aikens, S.P. Webb, R.L. Bell, G.D. Fletcher, M.W. Schmidt, M.S. Gordon, A derivation of the frozen-orbital unrestricted open-shell and restricted closed-shell second-order perturbation theory analytic gradient expressions, *Theoret. Chem. Acc.* 110 (2003) 233–253.
- [14] R.G. Parr, W. Yang, *Density-Functional Theory of Atoms and Molecules*, Oxford University Press, USA, 1994.
- [15] J.P. Perdew, K. Burke, M. Ernzerhof, Generalized gradient approximation made simple, *Phys. Rev. Lett.* 77 (1996) 3865–3868.
- [16] C.T. Lee, W. Yang, R.G. Parr, Development of the Colle-Salvetti correlation-energy formula into a functional of the electron density, *Phys. Rev. B* 37 (1988) 785–789.
- [17] A.D. Boese, N.C. Handy, A new parametrization of exchange–correlation generalized gradient approximation functionals, *J. Chem. Phys.* 114 (2001) 5497–5503.
- [18] J.B. Foresman, A.E. Frisch, *Exploring Chemistry with Electronic Structure Methods*, 2nd ed., Gaussian, Inc., Pittsburgh, USA, 1996.

- [19] F.A. Hamprecht, A.J. Cohen, D.J. Tozer, N.C. Handy, Development and assessment of new exchange-correlation functionals, *J. Chem. Phys.* 109 (1998) 6264–6271.
- [20] T.H. Dunning Jr., Gaussian basis sets for use in correlated molecular calculations. I. The atoms boron through neon and hydrogen, *J. Chem. Phys.* 90 (1989) 1007–1023.
- [21] D.E. Woon, T.H. Dunning Jr., Gaussian basis sets for use in correlated molecular calculations. III. The atoms aluminum through argon, *J. Chem. Phys.* 98 (1993) 1358–1371.
- [22] W.R. Wadt, P.J. Hay, Ab initio effective core potentials for molecular calculation, potentials for main group elements Na to Bi, *J. Phys. Chem.* 82 (1985) 284–298.
- [23] W.P. Hu, D.G. Truhlar, Structural distortion of CH<sub>3</sub>I in an ion-dipole precursor complex, *J. Phys. Chem.* 98 (1994) 1049–1952.
- [24] K.A. Peterson, B.C. Shepler, D. Figgen, H. Stoll, On the spectroscopic and thermochemical properties of ClO, BrO, IO and their anions, *J. Phys. Chem. A* 110 (2006) 13877–13883.
- [25] NWChem user manual, <http://www.nwchem-sw.org/index.php/NWChem.Documentation>
- [26] F. Jensen, Introduction to Computational Chemistry, 2nd ed., John Wiley & Sons, Ltd., 2007.
- [27] M. Valiev, E.J. Bylaska, N. Govind, K. Kowalski, T.P. Straatsma, H.J.J. van Dam, D. Wang, J. Nieplocha, E. Apra, T.L. Windus, W.A. de Jong, NWChem: A comprehensive and scalable open-source solution for large scale molecular simulations, *Comput. Phys. Commun.* 181 (2010) 1477–1489.
- [28] A. Szabo, N.S. Ostlund, Modern Quantum Chemistry, Introduction to Advanced Electronic Structure Theory, Dover Publications, Inc., USA, 1996.
- [29] B. Ruscic, Private communication of unpublished Active Thermochemical Tables (ATcT) values using ver. 1.118 of the Thermochemical Network.
- [30] B. Ruscic, R.E. Pinzon, M.L. Morton, G. von Laszewski, S. Bittner, S.G. Nijssure, K.A. Amin, M. Minkoff, A.F. Wagner, *J. Phys. Chem. A* 108 (2004) 9979–9997.
- [31] B. Ruscic, R.E. Pinzon, G. von Laszewski, D. Kodeboyina, A. Burcat, D. Leahy, D. Montoya, A.F. Wagner, *J. Phys. Conf. Ser.* 16 (2005) 561–570.
- [32] J.P. Merrick, D. Moran, L. Radom, An evaluation of harmonic vibrational frequency scale factors, *J. Phys. Chem. A* 111 (2007) 11683–11700.
- [33] J.L. Duncan, A. Allan, D.C. McKean, <sup>13</sup>C frequency shifts and the general harmonic force fields of methyl chloride, bromide and iodide, *Mol. Phys.* 18 (1970) 289–303.
- [34] M.M. Law, J.L. Duncan, I.M. Mills, The general harmonic force field of methyl fluoride, *J. Mol. Struct.* 260 (1992) 323–331.
- [35] C. Li, P. Ross, J.E. Szulejko, T.B. McMahon, High-pressure mass spectrometric investigations of the potential energy surfaces of gas-phase SN<sub>2</sub> reactions, *J. Am. Chem. Soc.* 118 (1996) 9360–9367.
- [36] M.N. Glukhovtsev, A. Pross, L.J. Radom, Gas-phase non-identity SN<sub>2</sub> reactions of halide anions with methyl halides: a high-level computational study, *J. Am. Chem. Soc.* 118 (1996) 6273–6284.
- [37] K.A. Peterson, D.E. Woon, T.H. Dunning Jr., *J. Chem. Phys.* 100 (1994) 7410–7415.
- [38] J. Zhang, J. Mikosch, S. Trippel, R. Otto, M. Weidemuller, R. Wester, W.L. Hase, F<sup>-</sup> + CH<sub>3</sub>I → FCH<sub>3</sub> + I<sup>-</sup> Reaction dynamics. nontraditional atomistic mechanisms and formation of a hydrogen-bonded complex, *J. Phys. Chem. Lett.* 1 (2010) 2747–2752.
- [39] A.D. Becke, Density-functional thermochemistry. III. The role of exact exchange, *J. Chem. Phys.* 98 (1993) 5648–5652.
- [40] A.D. Becke, Density-functional exchange-energy approximation with correct asymptotic behavior, *Phys. Rev. A* 38 (1988) 3098–3100.
- [41] J.P. Perdew, Y. Wang, Accurate and simple analytic representation of the electron-gas correlation energy, *Phys. Rev. B* 45 (1992) 13244–13249.
- [42] Y. Zhao, D.G. Truhlar, The M06 suite of density functionals for main group thermochemistry, thermochemical kinetics, noncovalent interactions, excited states, and transition elements: two new functionals and systematic testing of four M06-class functionals and 12 other functionals, *Theor. Chem. Acc.* 120 (2008) 215–241.